

# Improved bounds on $W$ - $W'$ mixing with ATLAS resonant $WZ$ production data at the LHC at $\sqrt{s} = 13$ TeV

I. A. Serenkova\*

*The Abdus Salam ICTP Affiliated Centre, Technical University of Gomel, 246746 Gomel, Belarus*

P. Osland†

*Department of Physics and Technology, University of Bergen, Postboks 7803, N-5020 Bergen, Norway*

A. A. Pankov‡

*The Abdus Salam ICTP Affiliated Centre, Technical University of Gomel, 246746 Gomel, Belarus*

*Institute for Nuclear Problems, Belarusian State University, 220030 Minsk, Belarus and*

*Joint Institute for Nuclear Research, Dubna 141980 Russia*

(Dated: March 9, 2022)

New charged vector bosons  $W'$  decaying into gauge boson pairs  $WZ$  are predicted in many scenarios of new physics, including models with an extended gauge sector (EGM). Due to the large variety of models (other unification groups, models with Supersymmetry, Little Higgs Models, Extra Dimensions) the more general EGM approach is here considered. For what concerns  $W'$ -production, these models are parametrised by two parameters, the  $W'$  mass  $M_{W'}$  and the  $W$ - $W'$  mixing parameter  $\xi$ . The diboson  $WZ$  production allows to place stringent constraints on this mixing angle and the  $W'$  mass, which we determine and present for the first time by using data from  $pp$  collisions at  $\sqrt{s} = 13$  TeV recorded by the ATLAS detector at the CERN LHC, with integrated luminosity of  $36.1 \text{ fb}^{-1}$ . By comparing the experimental limits to the theoretical predictions for the total cross section of  $W'$  resonant production and its subsequent decay into  $WZ$  pairs, we show that the derived constraints on the mixing angle are rather severe, between  $10^{-4}$  and  $10^{-3}$ , i.e., greatly improved with respect to those derived from the global analysis of electroweak data which yield  $\xi \lesssim 10^{-2}$ . We combine the limits derived from  $WZ$  production data with those obtained from the  $W' \rightarrow e\nu$  process in order to significantly extend the exclusion region in the  $M_{W'}\text{--}\xi$  parameter plane and obtain the most stringent exclusion limits to date. We present the combined allowed parameter space for the EGM  $W'$  boson after incorporating indirect constraints from low energy electroweak data, direct search constraints from Tevatron and from the LHC Run I with 7 and 8 TeV as well as at Run II with 13 TeV data.

---

\* Inna.Serenkova@cern.ch

† Per.Osland@uib.no

‡ pankov@ictp.it

## I. INTRODUCTION. THE $W'$ EGM AS A GENERAL APPROACH

Many extensions to the Standard Model (SM) predict the existence of charged and neutral, heavy gauge bosons that could be discovered at the Large Hadron Collider (LHC). In the simplest models these particles are considered copies of the SM  $W$  and  $Z$  bosons and are commonly referred to as  $W'$  and  $Z'$  bosons [1]. The Sequential Standard Model (SSM) [2] posits a  $W'_{\text{SSM}}$  boson with couplings to fermions that are identical to those of the SM  $W$  boson but for which the coupling to  $WZ$  is absent. The SSM has been used as a reference point for experimental  $W'$  boson searches for decades, the results can be re-interpreted in the context of other models of new physics, and it is useful for comparing the sensitivity of different experiments.

At the LHC, a promising way to search for heavy  $W'$  bosons is through their single production as an  $s$ -channel resonance with their subsequent leptonic decays

$$pp \rightarrow W'X \rightarrow \ell\nu X, \quad (1)$$

where in what follows,  $\ell = e, \mu$  unless otherwise stated. The Feynman diagram for the  $W'$  boson production and its dilepton decay at the parton level is illustrated in Fig. 1. This process (1) offers the simplest event topology for the discovery of a  $W'$  with a large production rate and a clean experimental signature. These channels are among the most promising early discoveries at the LHC [3, 4]. There have also been many theoretical studies of  $W'$  boson searches [5–14] at the LHC.

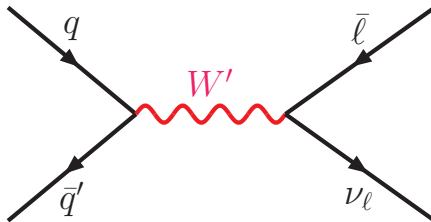


FIG. 1. Leading-order (LO) Feynman diagram of  $W'$  boson production and dilepton decay. The final state shown denotes both the  $(\bar{\ell}\nu_\ell)$  state and its charge conjugated one.

The ATLAS and CMS collaborations set limits on the  $W'$  production cross section times branching fraction in the process (1),  $\sigma(pp \rightarrow W'X) \times \text{BR}(W' \rightarrow \ell\nu)$ , for  $M_{W'}$  in the 0.15 TeV – 6 TeV range. The most stringent limits on the mass of a  $W'_{\text{SSM}}$  boson to date come from the searches in the  $W' \rightarrow e\nu$  and  $W' \rightarrow \mu\nu$  channels by the ATLAS and CMS collaborations using data taken at  $\sqrt{s} = 13$  TeV. The ATLAS and CMS analyses were based on data corresponding to an integrated luminosity of 36.1 fb $^{-1}$  and 35.9 fb $^{-1}$  and set a 95% confidence level (CL) lower limit on the  $W'_{\text{SSM}}$  mass of 5.2 TeV [3, 4].

An alternative  $W'$  search channel is the diboson one

$$pp \rightarrow W'X \rightarrow WZX. \quad (2)$$

The study of gauge boson pair production offers a powerful test of the spontaneously broken gauge symmetry of the SM and can be used as a probe for new phenomena beyond the SM.

Massive resonances that can decay to gauge boson pairs are predicted by many scenarios of new physics, including extended gauge models (EGM) [2, 15], models of warped extra dimensions [16, 17], technicolour models [18, 19] associated with the existence of technirho and other technimesons, and more generic composite Higgs models [20–22], etc. Searches for exotic heavy particles that decay into  $WZ$  pairs are complementary to searches in the leptonic channels  $\ell\nu$  of process (1). Moreover, there are models in which the  $W'$  couplings to SM fermions are suppressed, giving rise to a fermiophobic  $W'$  with an enhanced coupling to  $W$  and  $Z$  bosons [1, 23]. It is therefore important to search for  $W'$  bosons also in the  $WZ$  final state.

Given the large variety of models which predict new heavy charged gauge bosons, it is a natural approach to use a simplified ansatz for such a search [24]. After a discovery of signatures associated to a new boson, detailed studies can be carried out to distinguish between these models and to determine whether the boson belongs to one of the theoretically motivated models such as an EGM, models of warped extra dimensions, technicolour, composite Higgs models, a Little Higgs model, a Left-Right Symmetric model or a totally different one. Following the traditions of direct searches at hadron colliders, such studies are based on the model first proposed in Ref. [2].

As mentioned above, in the SSM, the coupling constants of the  $W'$  boson with SM fermions are the direct transcription of the corresponding SM couplings, while the  $W'$  coupling to  $WZ$  is absent,  $g_{W'WZ} = 0$  [25, 26]. Note that

this suppression may arise in an EGM in a natural manner: if the new gauge bosons and the SM ones belong to different gauge groups, a vertex such as  $W'WZ$  is forbidden. They can only occur after symmetry breaking due to mixing of the gauge eigenstates. Triple gauge boson couplings (such as  $W'WZ$ ) as well as the vector-vector-scalar couplings (like  $W'WH$ ) arise from the symmetry breaking and may contribute to the  $W'$  decay. The vertices are then suppressed by a factor of the order of  $(M_W/M_{W'})^2$ .

Heavy spin-1 resonances are a generic prediction of many EGMs. In particular, the EGM introduces extra, heavy, charged  $W'$  and neutral  $Z'$  bosons with SM couplings to fermions and with modified  $W$ - $W'$  mixing-induced coupling of the heavy  $W'$  to  $WZ$ . Here, we concentrate on a study of these mixing effects in the decay of  $W'$  to  $WZ$ .<sup>1</sup>

In an EGM, the trilinear gauge boson coupling is modified by a mixing factor

$$\xi = \mathcal{C} \times (M_W/M_{W'})^2, \quad (3)$$

where  $\mathcal{C}$  is a scaling constant that sets the coupling strength. Note that the EGM can be parametrized either in terms of  $(M_{W'}, \mathcal{C})$  or in terms of  $(M_{W'}, \xi)$ . Specifically, in an EGM the standard-model trilinear gauge boson coupling strength  $g_{WWZ}$  ( $= e \cot \theta_W$ ), is replaced by  $g_{W'WZ} = \xi \cdot g_{WWZ}$ . Following the parametrization of the trilinear gauge boson coupling  $W'WZ$  presented in [30] for the analysis and interpretation of the CDF data on  $p\bar{p} \rightarrow W'X \rightarrow WZX$ , expressed in terms of two free parameters,<sup>2</sup>  $\xi$  and  $M_{W'}$ , we will set, for the first time,  $W'$  limits as functions of the mass  $M_{W'}$  and mixing factor  $\xi$  by using the ATLAS resonant diboson production data [31] collected at a center of mass energy of  $\sqrt{s} = 13$  TeV. The presented analysis in the EGM with two free parameters is more general than the previous ones where the only parameter is the  $W'$  mass. As to the SSM, we have  $W'_{\text{SSM}} \equiv W'_{\text{EGM}}(\xi = 0)$ .

Previous searches for an EGM  $W'$  resonance in the  $WZ$  channel have been carried out using  $p\bar{p}$  collision data at  $\sqrt{s} = 1.96$  TeV at the Tevatron and  $pp$  collision data at  $\sqrt{s} = 7$  and 8 TeV at the LHC. Early results from the Tevatron [30, 32] derived by the CDF and D0 collaborations have put limits, at the 95% CL, on the mass of a  $W'$  boson between 285 and 516 GeV and between 188 and 520 GeV, respectively. The ATLAS and CMS collaborations have also set exclusion bounds on the production and decay of a  $W'$  boson, in searches using the  $\ell\nu\ell'\ell'$  channel, the ATLAS [33] and CMS [34] collaborations have excluded, at the 95% CL, EGM ( $\mathcal{C} = 1$ )  $W'$  bosons decaying to  $WZ$  for  $W'$  masses below 1.52 TeV and 1.55 TeV, respectively. Here  $\ell'$  stands for an electron or muon. In addition the ATLAS Collaboration has excluded EGM ( $\mathcal{C} = 1$ )  $W'$  bosons for masses below 1.59 TeV using the  $\ell\ell qq$  [25] channel, and below 1.49 TeV using the  $\ell\nu qq$  [35] channel. These have also been excluded with masses between 1.3 and 1.5 TeV and below 1.7 TeV by the ATLAS [36] and CMS [37] collaborations, respectively, using the fully hadronic final state. To improve the sensitivity to new diboson resonances in the context of the EGM ( $\mathcal{C} = 1$ ) in order to set the strongest exclusion bounds on the  $W'$  masses, the fully leptonic, semi-leptonic and fully hadronic channels at 8 TeV were combined [26]. The result of this combination was interpreted using the EGM  $W'$  model with  $\mathcal{C} = 1$  as a benchmark. The observed lower limit on the  $W'$  mass was found to be 1.8 TeV. The various decay channels generally differ in sensitivity in different mass regions. The fully leptonic channel, in spite of a lower branching ratio, is expected to be particularly sensitive to low-mass resonances as it has lower backgrounds.

The strongest lower limit on the  $W'$  mass set at 13 TeV is  $M_{W'} > 3.2$  TeV [1] in the context of the heavy vector-triplet (HVT) model of “weekly-coupled scenario A” [38]. The HVT generalises a large number of models that predict spin-1 charged ( $W'$ ) and neutral ( $Z'$ ) resonances. Such models can be described in terms of just a few parameters: two coefficients  $c_F$  and  $c_H$ , scaling the couplings to fermions, and to the Higgs and longitudinally polarized SM vector bosons respectively, and the strength  $g_V$  of the new vector boson interaction. Two benchmark models are considered in the HVT scenario. We are interested in one of them, referred to as HVT model-A, with  $g_V = 1$  because of its similarity to the EGM ( $\mathcal{C} = 1$ )  $W'$  model, that have comparable branching fractions to fermions and gauge bosons.

Limits were also set on the EGM  $W'$  boson coupling strength scaling factor  $\mathcal{C}$ , as functions of  $M_{W'}$ , within the EGM framework [30, 32, 34, 39, 40]. It was shown that if the coupling between the  $W'$  boson and  $WZ$  happens to be stronger (weaker) than that predicted by the EGM with  $\mathcal{C} = 1$ , the observed and expected limits will be more stringent (relaxed).

The properties of  $W'$  bosons are also constrained by measurements of EW processes at low energies, i.e., at energies much below the mass  $M_{W'}$ . Such bounds on the  $W$ - $W'$  mixing are mostly due to the change in  $W$  properties compared to the SM predictions. These measurements show that the mixing angle  $\xi$  between the gauge eigenstates must be smaller than about  $10^{-2}$  [1].

In this work, we derive bounds on a possible new charged spin-1 resonance ( $W'$ ) in the EGM framework from the available ATLAS data on  $WZ$  pair production [31]. The search was conducted for a new  $W'$  resonance decaying into a  $WZ$  boson pair, where the  $W$  boson decays leptonically ( $W \rightarrow \ell\nu$  with  $\ell = e, \mu$ ) and the  $Z$  boson decays hadronically

<sup>1</sup> Analogous analysis of the  $Z$ - $Z'$  mixing proposed in [27] and recently performed on the basis of resonant diboson production data in  $pp \rightarrow Z'X \rightarrow W^+W^-X$  at the ATLAS and CMS can be found in e.g. [28, 29].

<sup>2</sup> Such a  $W'$ , described in terms of two parameters is here referred to as the EGM boson.

( $Z \rightarrow q\bar{q}$  with  $q$  quarks). We present results as constraints on the relevant  $W$ - $W'$  mixing angle  $\xi$  and on the mass  $M_{W'}$  and display the combined allowed parameter space for the EGM  $W'$  boson, showing also indirect constraints from electroweak precision data (EW), direct search constraints from the Tevatron and from the LHC with 7 and 8 TeV as well as with 13 TeV data.

The paper is organized as follows. In Sec. II we summarize the relevant cross section and study the  $W' \rightarrow WZ$  width in the EGM. Then, in Sec. III we show the resulting constraints on the  $M_{W'}\text{-}\xi$  parameter space obtained from diboson and dilepton processes. In Sec. IV we collect and compare the indirect constraints obtained from electroweak precision data, direct search constraints derived from the diboson process at the Tevatron and at the LHC. Also, we explore the role of the dilepton process in reducing the excluded area in the  $W'$  parameter plane, and in Sec. V we conclude.

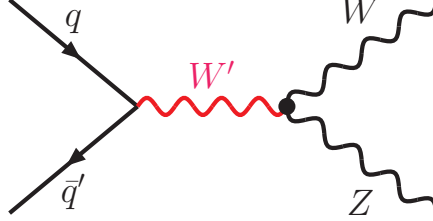


FIG. 2. Lowest-order Feynman diagram for the  $W'$  boson production and decay to the diboson  $WZ$  final state.

## II. $W'$ PRODUCTION AND DECAY AT THE LHC

At lowest order within the EGM,  $W'$  production and decay into  $WZ$  in proton-proton collisions occurs through quark-antiquark interactions in the  $s$ -channel, as illustrated by the Feynman diagram shown in Fig. 2.<sup>3</sup> The cross section of process (2) at the LHC can be observed through resonant pair production of gauge bosons  $WZ$ . Using the narrow width approximation (NWA), one can factorize the process (2) into the  $W'$  production and the  $W'$  decay,

$$\sigma(pp \rightarrow W'X \rightarrow WZX) = \sigma(pp \rightarrow W'X) \times \text{BR}(W' \rightarrow WZ). \quad (4)$$

Here,  $\sigma(pp \rightarrow W'X)$  is the total (theoretical)  $W'$  production cross section and  $\text{BR}(W' \rightarrow WZ) = \Gamma_{W'}^{WZ}/\Gamma_{W'}$  with  $\Gamma_{W'}$  the total width of  $W'$ . The cross section  $\sigma(pp \rightarrow W'X)$  for the inclusive  $W'$  production  $pp \rightarrow W'X$  is derived from the quark subprocess  $q\bar{q}' \rightarrow W'$  which can be written as [41]:

$$\hat{\sigma}(q\bar{q}' \rightarrow W') = \frac{\pi |V_{qq'}|^2}{4} g^2 \delta(\hat{s} - M_{W'}^2). \quad (5)$$

Here, the weak coupling constant  $g = e/\sin\theta_W$ , and  $V_{qq'}$  is the Cabibbo-Kobayashi-Maskawa (CKM) matrix element connecting quark  $q$  and antiquark  $\bar{q}'$ . The hadronic cross section can be obtained by the summation over all contributing quark-antiquark combinations and integration over the momentum fractions [2, 42],

$$\sigma(p_1 p_2 \rightarrow W'X) = \frac{K}{3} \int_0^1 dx_1 \int_0^1 dx_2 \sum_{q, \bar{q}'} [f_{q|p_1}(x_1, M_{W'}^2) f_{\bar{q}'|p_2}(x_2, M_{W'}^2)] \hat{\sigma}(q\bar{q}' \rightarrow W'). \quad (6)$$

With  $\hat{s}$  the parton subprocess c.m. energy squared, and  $s$  the proton-proton c.m. energy squared, it is assumed that  $\hat{s} = x_1 x_2 s = M_{W'}^2$  is the appropriate scale of the quark distributions. The coefficient of  $1/3$  in front of Eq. (6) is a color factor. Furthermore,  $f_{q|p_1}(x_1, M_{W'}^2)$  and  $f_{\bar{q}'|p_2}(x_2, M_{W'}^2)$  are quark and antiquark momentum distribution functions for the two protons, with  $x_{1,2}$  the parton fractional momenta, related to the rapidity  $y$  via  $x_{1,2} = (M_{W'}/\sqrt{s}) \exp(\pm y)$ . The  $K$  factor accounts for higher-order QCD contributions. For the numerical computation, we use the CTEQ-6L1 parton distributions [43] with the factorization and renormalization scales  $\mu_F^2 = \mu_R^2 = M_{W'}^2 = \hat{s}$ . The obtained

<sup>3</sup> This may however be considered an *effective* diagram, in the sense that an underlying theory may generate the  $W'WZ$  vertex at loop order.

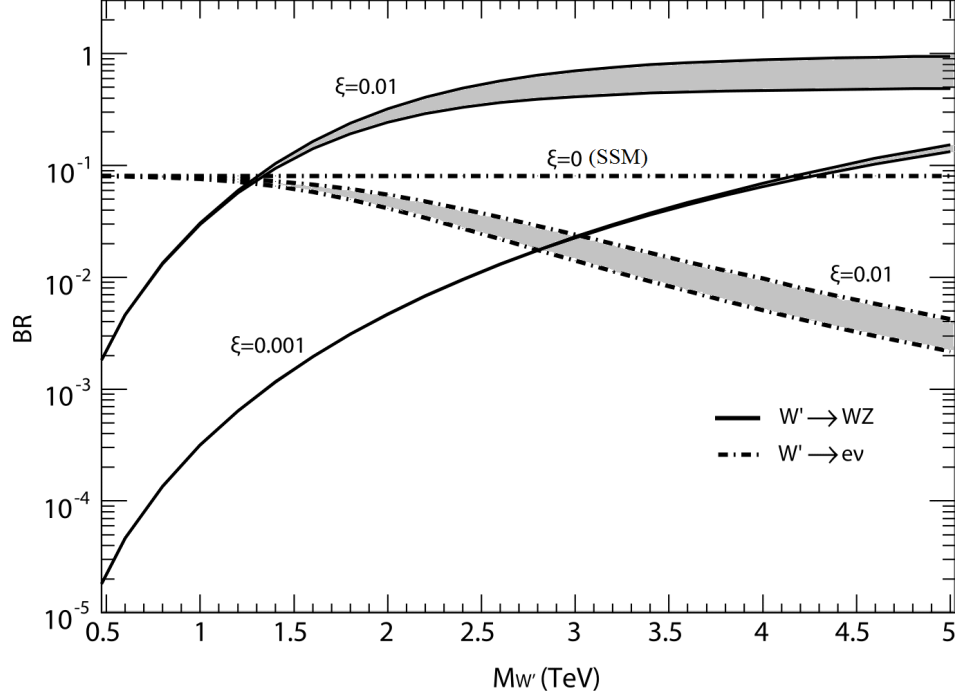


FIG. 3. Branching fraction  $\text{BR}(W' \rightarrow WZ)$  (solid) vs  $M_{W'}$  in the EGM for non-zero  $W$ - $W'$  mixing factor  $\xi = 10^{-3}$  and  $10^{-2}$ . For the  $W' \rightarrow e\nu$  mode (dot-dashed),  $\text{BR}(W' \rightarrow e\nu)$  for  $\xi = 0$  ( $W'_{\text{SSM}}$ ) and  $\xi = 0.01$  ( $W'_{\text{EGM}}$ ) are shown. The shaded bands indicate the uncertainty resulting from the inclusion of the  $WH$  decay mode, the upper and lower bounds correspond to the assumptions  $\Gamma_{W'}^{WH} = 0$  and  $\Gamma_{W'}^{WH} = \Gamma_{W'}^{WZ}$ , respectively.

constraints presented in the following are numerically not significantly modified when  $\mu_{F,R}$  is varied in the range from  $\mu_{F,R}/2$  to  $2\mu_{F,R}$ .

In the EGM the  $W'$  bosons can decay into the SM fermions, gauge bosons ( $WZ$ ), or a pair of an SM boson and a Higgs boson. In the calculation of the total width  $\Gamma_{W'}$ , we consider the following channels:  $W' \rightarrow f\bar{f}'$ ,  $WZ$ , and  $WH$ , where  $H$  is the SM Higgs boson and  $f$  are the SM fermions ( $f = \ell, \nu, q$ ). In this study only left-handed neutrinos are considered while possible right-handed neutrinos are assumed to be kinematically unavailable as final states. Also, throughout the paper we shall ignore the couplings of the  $W'$  to beyond-SM particles such as SUSY partners and any exotic fermions in the theory, which may increase the width of the  $W'$  and hence lower the branching ratio into a  $WZ$  pair. As a result, the total decay width of the  $W'$  boson is taken to be

$$\Gamma_{W'} = \sum_f \Gamma_{W'}^{f\bar{f}'} + \Gamma_{W'}^{WZ} + \Gamma_{W'}^{WH}. \quad (7)$$

The presence of the two last decay channels, which are often neglected at low and moderate values of  $M_{W'}$ , is due to  $W$ - $W'$  mixing which is constrained to be tiny. In particular, for the range of  $M_{W'}$  values below  $\sim 1.0 - 1.5$  TeV, the dependence of  $\Gamma_{W'}$  on the values of  $\xi$  (within its allowed range) induced by  $\Gamma_{W'}^{WZ}$  and  $\Gamma_{W'}^{WH}$  is unimportant because  $\sum_f \Gamma_{W'}^{f\bar{f}'}$  dominates over diboson partial widths. Therefore, in this mass range, one can approximate the total width as  $\Gamma_{W'} \approx \sum_f \Gamma_{W'}^{f\bar{f}'}$ , where the sum runs over SM fermions only.

Due to the assumption that the  $W'$  and the  $W$  have identical couplings to the SM fermions, the total  $W'$  width can be expressed in terms of the  $W$  width  $\Gamma_W$ . For  $W'$  masses below  $m_t + m_b \simeq 180$  GeV the kinematically allowed decay channels are identical for the SM  $W$  and the total width reads as  $\Gamma_{W'} = (M_{W'}/M_W) \Gamma_W$ . For  $W'$  masses above 180 GeV the decay  $W' \rightarrow t\bar{b}$  opens. Since the phase space is enlarged it results in an increase of the  $W'$  width by a factor of  $4/3$ , namely  $\Gamma_{W'} = (4M_{W'}/3M_W) \Gamma_W$ . In this  $W'$  mass range limited by the upper bound of about 1.5 TeV, a predicted branching fraction  $\text{BR}(W' \rightarrow l\nu) = 1/12$  (or about 8.2%) for each of the leptonic channels studied, as illustrated in Fig. 3 for the case of vanishing  $W$ - $W'$  mixing ( $\xi = 0$ ). Under these assumptions (for decays to massless SM fermions), the total width scales with the mass as  $\Gamma_{W'} = (g^2/4\pi)M_{W'}$  [41]. Allowing also for final-state QED and QCD corrections, one arrives at  $\Gamma_{W'} \approx 3.5\% \times M_{W'}$  (see, e.g. [44]).

For heavier  $W'$  bosons, the diboson decay channels,  $WZ$  and  $WH$ , start to play an important role because of their significant contribution to the  $W'$  total decay width,  $\Gamma_{W'}$ , and to the branching ratio  $\text{BR}(W' \rightarrow WZ)$ , we are no longer able to ignore them. To be specific, we take an approach as model-independent as possible, and for numerical illustration show our results in two simple scenarios. In the first scenario, we treat the model as effectively having a suppressed partial width of  $W' \rightarrow WH$  with respect to that of  $W' \rightarrow WZ$ , i.e.  $\Gamma_{W'}^{WH} \ll \Gamma_{W'}^{WZ}$ , so that one can ignore the former, taking  $\Gamma_{W'}^{WH} \simeq 0$ . In this case, numerical results with our treatment will serve as an upper bound on the size of the signal. The second scenario assumes that both partial widths are comparable,  $\Gamma_{W'}^{WH} \simeq \Gamma_{W'}^{WZ}$  for heavy  $M_{W'}$  as required by the equivalence theorem [45]. In particular, the equivalence theorem requires that  $W'$  decays into fields that are part of the same Higgs doublet (e.g., longitudinal  $Z$  and  $H$ ) have equal decay widths up to electroweak symmetry breaking effects and phase-space factors [10]. While the equivalence theorem might suggest a value for  $\text{BR}(W' \rightarrow WH)$  comparable to  $\text{BR}(W' \rightarrow WZ)$ , the  $W'WH$  coupling is actually quite model dependent [10]. In the numerical analysis presented below, we will consider both scenarios. In the second scenario,  $\Gamma_{W'}$  would be larger, with a suppression of the branching ratio to  $WZ$ , and the bounds from LHC (and the ability for observing the  $W$ - $W'$  mixing effect) would be reduced.

Note also that for all  $M_{W'}$  values of interest for LHC the width of the  $W'$  boson is considerably smaller than the experimental mass resolution  $\Delta M$  ( $M \equiv \sqrt{s}$ ) for which we adopt the parametrization in reconstructing the diboson invariant mass of the  $WZ$  system,  $\Delta M/M \approx 5\%$ , as proposed, e.g., in [46, 47]. This condition validates the NWA adopted in this work.

The expression for the partial width of the  $W' \rightarrow WZ$  decay channel in the EGM can be written as [2]:

$$\Gamma_{W'}^{WZ} = \frac{\alpha_{\text{em}}}{48} \cot^2 \theta_W M_{W'} \frac{M_{W'}^4}{M_W^2 M_Z^2} \left[ \left( 1 - \frac{M_Z^2 - M_W^2}{M_{W'}^2} \right)^2 - 4 \frac{M_W^2}{M_{W'}^2} \right]^{3/2} \times \left[ 1 + 10 \left( \frac{M_W^2 + M_Z^2}{M_{W'}^2} \right) + \frac{M_W^4 + M_Z^4 + 10 M_W^2 M_Z^2}{M_{W'}^4} \right] \cdot \xi^2. \quad (8)$$

As one can see from Eqs. (7) and (8), in the first scenario where  $\Gamma_{W'}^{WH} = 0$ , for a fixed mixing factor  $\xi$  and at large  $M_{W'}$ , where  $\Gamma_{W'}^{WZ}$  dominates over  $\sum_f \Gamma_{W'}^{f\bar{f}'}$ , the total width increases rapidly with the  $W'$  mass because of the quintic dependence on the  $M_{W'}$  mass of the  $WZ$  mode,  $\Gamma_{W'}^{WZ} \propto M_{W'} \cdot M_{W'}^4 / (M_W^2 M_Z^2)$ , which corresponds to the production of longitudinally polarized  $W$  and  $Z$  in the decay channel  $W' \rightarrow W_L Z_L$ . In this case, the  $WZ$  mode becomes dominant and  $\text{BR}(W' \rightarrow WZ) \rightarrow 1$ , while the fermionic decay channels ( $\sum_f \Gamma_{W'}^{f\bar{f}'} \propto M_{W'}$ ) are increasingly suppressed. However, in the second scenario with  $\Gamma_{W'}^{WH} = \Gamma_{W'}^{WZ}$ ,  $\text{BR}(W' \rightarrow WZ) \rightarrow 0.5$  when  $M_{W'}$  increases, as is demonstrated in Fig. 3, in particular for larger allowed value of the mixing factor,  $\xi = 0.01$ . Also, Fig. 3 shows that the branching ratio of  $W'$  to fermions, e.g.  $\text{BR}(W' \rightarrow e\nu)$ , decreases as  $\xi$  increases. This is opposite to the diboson decay mode of  $W' \rightarrow WZ$  where the branching ratio increases as  $\xi$  increases.

### III. CONSTRAINTS ON $W'$ FROM THE DIBOSON AND DILEPTON PROCESSES

#### A. $W$ - $W'$ mixing effects in $W' \rightarrow WZ$

Here, we present an analysis, employing the most recent measurements of diboson processes provided by ATLAS [31]. In Fig. 4, we show the observed and expected 95% C.L. upper limits on the production cross section times the branching fraction,  $\sigma_{95\%} \times \text{BR}(W' \rightarrow WZ)$ , as a function of the  $W'$  mass,  $M_{W'}$ . The expected upper limit set on the signal cross section is the greatest value of the signal cross section that is not excluded with 95% confidence. The data analyzed comprises  $pp$  collisions at  $\sqrt{s} = 13$  TeV, recorded by the ATLAS ( $36.1 \text{ fb}^{-1}$ ) detector [31] at the LHC. As mentioned above, ATLAS analyzed the  $WZ$  production in the process (2) through the semileptonic final states.

Then, for  $W'$  we compute the LHC theoretical production cross section multiplied by the branching ratio into  $WZ$  bosons,  $\sigma(pp \rightarrow W'X) \times \text{BR}(W' \rightarrow WZ)$ , as a function of the two parameters ( $M_{W'}$ ,  $\xi$ ), and compare it with the limits established by the ATLAS experiment,  $\sigma_{95\%} \times \text{BR}(W' \rightarrow WZ)$ . Our strategy in the present analysis is to adopt the SM backgrounds that have been carefully evaluated by the experimental collaboration and simulate only the  $W'$  signal. We set cross section limits on  $W'$  as functions of  $M_{W'}$  and  $\xi$ . Our results extend the sensitivity beyond the corresponding CDF Tevatron results [30, 32] as well as the ATLAS and CMS sensitivity attained at 7 and 8 TeV in [30, 32, 34, 39, 40]. Also, for the first time, we set  $W'_{\text{EGM}}$  limits as functions of mass  $M_{W'}$  and mixing factor  $\xi$  at the LHC from the 13 TeV data with a luminosity of  $36.1 \text{ fb}^{-1}$ .

In Fig. 4, the inner (green) and outer (yellow) bands around the expected limits represent  $\pm 1\sigma$  and  $\pm 2\sigma$  uncertainties, respectively. The simulation of signals for the EGM  $W'$  is based on an adapted version of the leading order (LO)

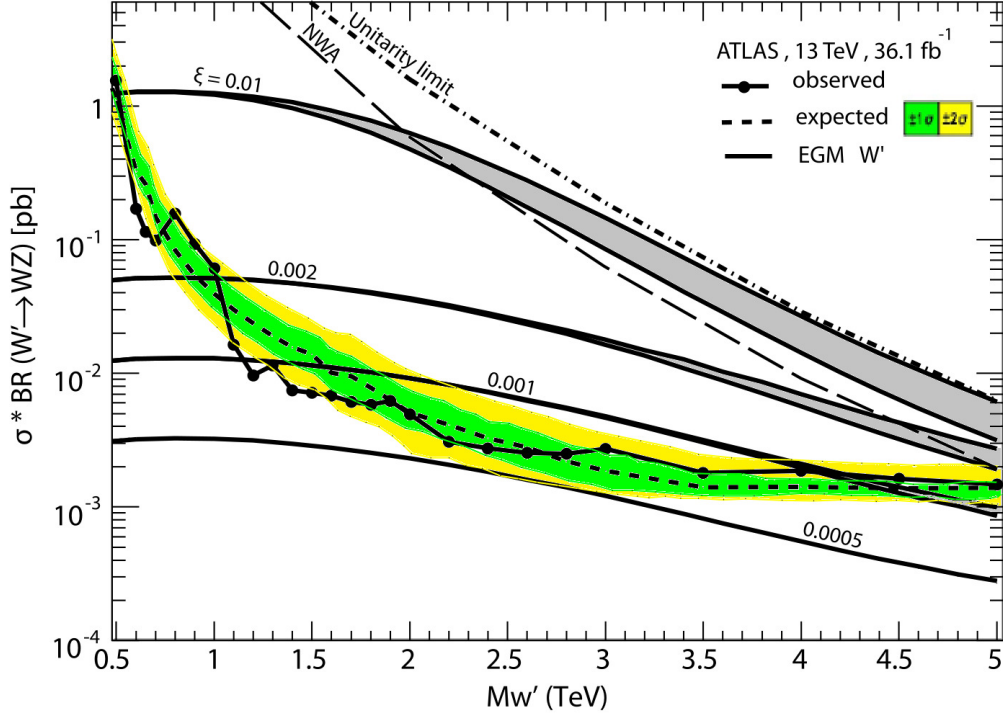


FIG. 4. Observed and expected 95% C.L. upper limits on the production cross section times the branching fraction,  $\sigma_{95\%} \times \text{BR}(W' \rightarrow WZ)$ , as a function of the  $W'$  mass,  $M_{W'}$ , showing ATLAS data for  $36.1 \text{ fb}^{-1}$  [31]. Theoretical production cross sections  $\sigma(pp \rightarrow W'X) \times \text{BR}(W' \rightarrow WZ)$  for the EGM are calculated from PYTHIA 8.2 with a  $W'$  boson mass-dependent  $K$ -factor used to correct for NNLO QCD cross sections, and given by solid curves, for mixing factor  $\xi$  ranging from 0.01 and down to 0.0005. The shaded bands are defined like in Fig. 3. The area lying below the long-dashed curve labelled by NWA corresponds to the region where the  $W'$  resonance width is predicted to be less than 5% of the resonance mass, in which the narrow-resonance assumption is satisfied. The lower boundary of the region excluded by the unitarity violation arguments is also indicated by the dot-dashed curve.

PYTHIA 8.2 event generator [48]. A mass-dependent  $K$  factor is used to rescale the LO PYTHIA prediction to the next-to-next-to-leading-order (NNLO) in  $\alpha_s$ . The theoretical  $W'$  production cross section  $\sigma(pp \rightarrow W'X)$  is scaled to a NNLO calculation in  $\alpha_s$  by ZWPROD [33, 35, 49], given by solid curves, and shown for mixing factor  $\xi$  ranging from 0.01 and down to 0.0005. The factorization and renormalization scales are set to the  $W'$  resonance mass.

As was explained in connection with Fig. 3, the upper (lower) boundary of the shaded areas correspond to a scenario where the contribution of the decay channel  $W' \rightarrow WH$  to the total  $W'$  decay width of Eq. (7) is  $\Gamma_{W'}^{WH} = 0$  ( $\Gamma_{W'}^{WH} = \Gamma_{W'}^{WZ}$ ). The area below the long-dashed curve labelled “NWA” corresponds to the region where the  $W'$  resonance width is predicted to be less than 5% of its mass, corresponding to the best detector resolution of the searches, where the narrow-resonance assumption is satisfied. In addition, in Fig. 4 we plot a curve labelled “Unitarity limit” that corresponds to the unitarity bound (see, e.g. [50] and references therein, where it was shown that the saturation of unitarity in the elastic scattering  $W^\pm Z \rightarrow W^\pm Z$  leads to the constraint  $g_{W'WZ\text{max}} = g_{WWZ} \cdot M_Z^2 / (\sqrt{3} M_{W'} M_W)$ ). This bound was obtained under the assumption that the couplings of the  $W'$  to quarks and to gauge bosons have the same Lorentz structure as those of the SM, but with a rescaled strength.

The theoretical curves for the cross sections  $\sigma(pp \rightarrow W'X) \times \text{BR}(W' \rightarrow WZ)$ , in descending order, correspond to values of the  $W$ - $W'$  mixing factor  $\xi$  from 0.01 to 0.0005. The intersection points of the expected (and measured) upper limits on the production cross section with these theoretical cross sections for various  $\xi$  give the corresponding lower bounds on  $(M_{W'}, \xi)$ , to be displayed below, in Sec. IV.

### B. $W$ - $W'$ mixing effects in $W' \rightarrow \ell\nu$

The above analysis was for the diboson process (2), employing one of the most recent ATLAS measurements [31]. Next, we turn to the dilepton production process (1), this process gives valuable complementary information. Unlike



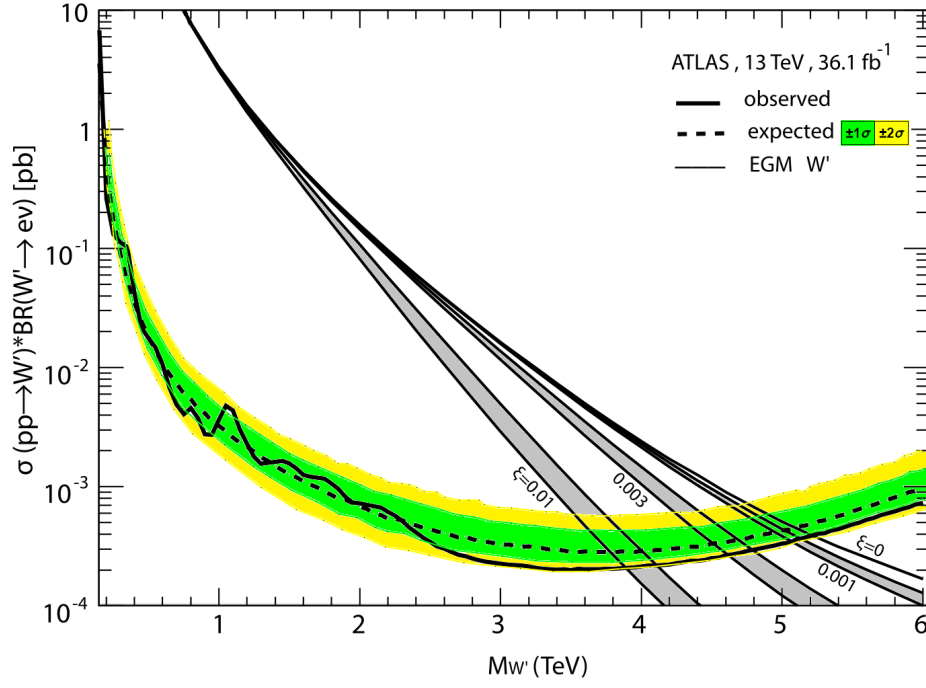


FIG. 5. Solid (dashed): observed (expected) 95% C.L. upper bound on the  $W'$  production cross section times branching ratio to two leptons,  $\sigma_{95\%} \times \text{BR}(W' \rightarrow e\nu)$ , obtained at the LHC with integrated luminosity  $\mathcal{L}_{\text{int}}=36.1 \text{ fb}^{-1}$  by the ATLAS collaboration [3]. Thin lines: theoretical production cross section  $\sigma(pp \rightarrow W'X) \times \text{BR}(W' \rightarrow e\nu)$  for the EGM  $W'$  boson, calculated from PYTHIA 8.2 with an NNLO  $K$  factor. These curves in descending order correspond to representative values of the  $W$ - $W'$  mixing factor  $\xi$  from 0 to 0.01. The shaded bands are defined like in Fig. 3.

the SSM, where there is no  $W$ - $W'$  mixing, in the EGM we consider a non-zero mixing  $\xi$  in the analysis of the  $W' \rightarrow e\nu$  process. As described in Sec. II, this results in a modification of  $\text{BR}(W' \rightarrow e\nu)$ .

We compute the  $W'$  production cross section at LO with PYTHIA 8.2 [48] at the LHC,  $\sigma(pp \rightarrow W'X)$ , multiplied by the branching ratio into two leptons,  $\ell\nu$  (here  $\ell = e$ ), i.e.,  $\sigma(pp \rightarrow W'X) \times \text{BR}(W' \rightarrow e\nu)$ , as a function of  $M_{W'}$ . A mass-dependent  $K$  factor is applied, based on NNLO QCD cross sections as calculated with FEWZ 3.1 [51, 52]. The  $K$ -factor varies approximately from 1.3 to 1.1 for the range of  $W'$  masses studied in this analysis, namely from 0.5 to 6.0 TeV. The NNLO corrections decrease with  $W'$  boson masses up to around 4.5 TeV [53]. For higher  $W'$  masses, the  $K$ -factor increases again and becomes similar to the low-mass values.

The product of the NNLO  $W'$  theoretical production cross section and branching fraction,  $\sigma(pp \rightarrow W'X) \times \text{BR}(W' \rightarrow e\nu)$ , for the  $W'$  boson for EGM strongly depends on the  $W'$  mass, and is for illustrative purposes given by thin solid curves, in descending order corresponding to values of the mixing factor  $\xi$  from 0.0 to 0.01, as displayed in Fig. 5. Further, we compare the theoretical cross section  $\sigma(pp \rightarrow W'X) \times \text{BR}(W' \rightarrow e\nu)$  with the upper limits of  $\sigma_{95\%} \times \text{BR}(W' \rightarrow e\nu)$  established by the ATLAS experiment [3] for  $36.1 \text{ fb}^{-1}$ . Qualitatively, the decrease of the theoretical cross section with increasing values of  $\xi$  can be understood as follows: For increasing  $\xi$ , the  $W' \rightarrow WZ$  mode will at high mass  $M_{W'}$  become more dominant (as illustrated in Fig. 3), and  $\text{BR}(W' \rightarrow e\nu)$  will decrease correspondingly.

Comparison of  $\sigma(pp \rightarrow W'X) \times \text{BR}(W' \rightarrow e\nu)$  vs  $\sigma_{95\%} \times \text{BR}(W' \rightarrow e\nu)$  displayed in Fig. 5 allows us to read off an allowed mixing for a given mass value, higher masses are allowed for smaller mixing, for the reason stated above. That comparison can be translated into constraints on the two-dimensional  $M_{W'}\text{-}\xi$  parameter plane, as will be shown in the next Sec. IV.

The above results are based on data corresponding to an integrated luminosity of  $36.1 \text{ fb}^{-1}$  taken by the ATLAS collaboration at  $\sqrt{s} = 13 \text{ TeV}$  in 2015 and 2016 [3]. However, recently the ATLAS collaboration presented preliminary results on searching for a  $W'$  boson conducted in the  $W' \rightarrow \ell\nu$  channel (1) based on  $79.8 \text{ fb}^{-1}$  of  $pp$  collision data collected in 2015 ( $3.2 \text{ fb}^{-1}$ ), 2016 ( $33.0 \text{ fb}^{-1}$ ) and 2017 ( $43.6 \text{ fb}^{-1}$ ) at a centre-of-mass energy of  $\sqrt{s} = 13 \text{ TeV}$  [54]. While the latter analysis followed closely the same procedure as in Ref. [3], the sensitivity of the search presented in [54] was improved due to the inclusion of the 2017 dataset. Specifically, this corresponds to an improvement of approximately  $\sim 0.5 \text{ TeV}$  in mass reach compared to the previous ATLAS analysis [3] which did not include the 2017



data and where a lower limit on the  $W'_{\text{SSM}}$  mass of 5.2 TeV was set at 95% CL. Those preliminary results have not been included in our present analysis.

#### IV. SUMMARIZING CONSTRAINTS ON THE $W$ - $W'$ MIXING

As described above, both the diboson mode and the dilepton process yield limits on the  $(M_{W'}, \xi)$  parameter space. These are rather complementary, as shown in Fig. 6, where we collect these and other limits for the considered EGM model. The limits arising from the diboson channel basically exclude large values of  $\xi$ , strongest at intermediate masses  $M_{W'} \sim 2 - 4$  TeV. The limits arising from the dilepton channel, on the other hand, basically exclude masses  $M_{W'} \lesssim 4 - 5.2$  TeV, with only a weak dependence on  $\xi$ . Also, we show the unitarity limits discussed above, as well as the upper bound for the validity of the NWA, indicated as dash-dotted and long-dashed lines, respectively.

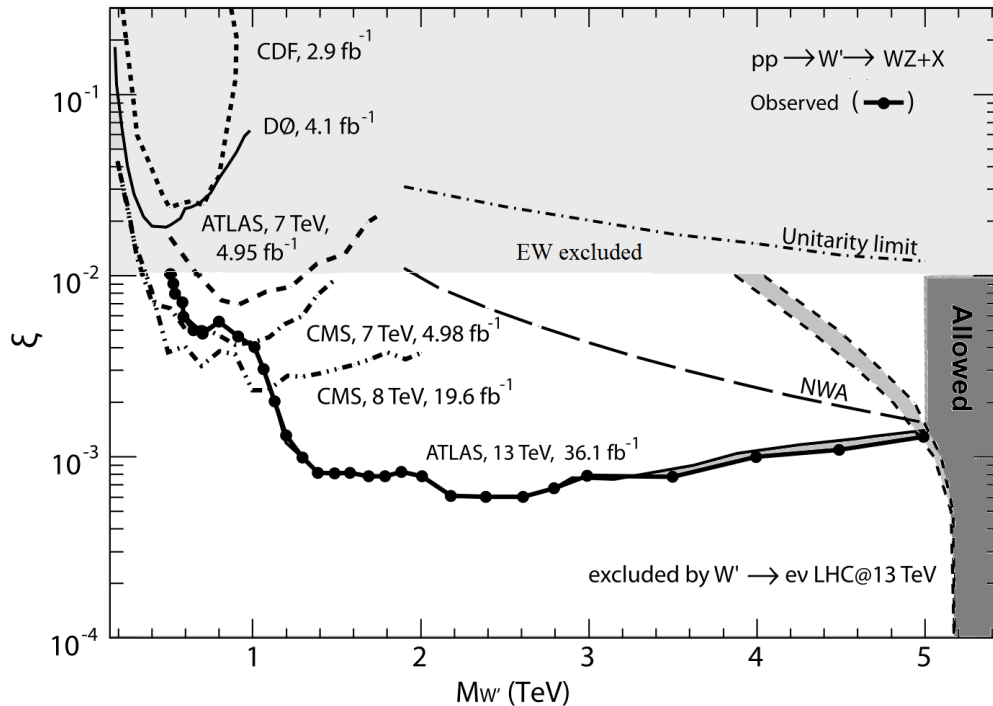


FIG. 6. 95% C.L. exclusion regions in the two-dimensional  $(M_{W'}, \xi)$  plane obtained after incorporating indirect constraints from electroweak precision data (the light shaded area at large  $\xi$ , labelled “EW excluded”), direct search constraints from the CDF and D0 collaborations (Tevatron) in  $p\bar{p} \rightarrow WZX$  as well as from the LHC with 7, 8 and 13 TeV from diboson  $W' \rightarrow WZ$  resonance search data in  $pp$  collisions. The region above each curve for the  $WZ$  channel is excluded. The steep curve labelled “excluded by  $W' \rightarrow e\nu$  LHC@13 TeV” shows the exclusion based on the dilepton channel  $pp \rightarrow e\nu X$ . The light shaded bands are defined like in Fig. 3. The unitarity limit and the upper bound for validity of the NWA are shown as dot-dashed and long-dashed curves, respectively. The overall allowed region is shown as a dark shaded area.

Interestingly, Fig. 6, which is dedicated to the EGM model, shows that at high  $W'$  masses, the limits on  $\xi$  obtained from the ATLAS diboson resonance production search at 13 TeV and at time-integrated luminosity of  $36.1 \text{ fb}^{-1}$  are substantially stronger than those derived from the low-energy electroweak data (EW), which are of order  $\sim 10^{-2}$  [1]. For completeness, we display limits on the  $W'$  parameters from the CDF and D0 (Tevatron) as well as from ATLAS and CMS obtained at 7 and 8 TeV of the LHC data taking in Run I. Fig. 6 shows that the experiments CDF and D0 at the Tevatron exclude EGM  $W'$  boson with  $\xi \gtrsim 2 \cdot 10^{-2}$  and  $0.6 \text{ TeV} < M_{W'} < 1 \text{ TeV}$  at the 95% C.L., whereas LHC in Run I improves those constraints excluding  $W'$  boson parameters at  $\xi \gtrsim 2 \cdot 10^{-3}$  in the mass range of  $0.6 \text{ TeV} < M_{W'} < 2 \text{ TeV}$ .<sup>4</sup>

<sup>4</sup> The latter ATLAS and CMS constraints depicted in Fig. 6 were obtained from resonant diboson production data collected at low energies, 7 and 8 TeV, by translating limits on the gauge coupling strength  $C$  vs  $M_{W'}$  [34, 39, 40] onto the  $M_{W'}$ - $\xi$  parameter plane, see Eq. (3).

In this note we combine the limits derived from  $WZ$  production data with those obtained from the  $W' \rightarrow e\nu$  process in order to significantly constrain the allowed region in the  $M_{W'}-\xi$  parameter space to obtain the most stringent exclusion limits to date, as illustrated in Fig. 6. It is interesting to note that for the EGM model under study the leptonic channel of (1) provides the strongest bound on much of the parameter space as shown in Fig. 6, which is based on the  $e\nu$  and  $WZ$  production data sets from the ATLAS experiment for time-integrated luminosity of  $36.1 \text{ fb}^{-1}$  at 13 TeV. In fact, the parameter space for the  $W'$  mass within the range of  $\sim 0.5 - 4 \text{ TeV}$  and  $\xi < 10^{-2}$  is basically excluded by  $W' \rightarrow e\nu$  process. In that mass range,  $WZ$  production plays a complementary role to the  $W' \rightarrow e\nu$  process, excluding  $W$ - $W'$  mixing above  $\xi \simeq 6 \cdot 10^{-4}$ . In addition, there is an area in parameter space within the  $W'$  mass region ranging approximately from 4 TeV to 5 TeV and lying below the “EW” boundary which is not excluded solely by the process of Eq. (1). The exclusion of that area is achieved with the process (2).

Furthermore, we could extrapolate the experimental sensitivity curves for the  $W' \rightarrow WZ$  decay channel for higher expected luminosity downwards by a factor of  $1/\sqrt{D}$ , for the  $M_{W'}$  mass range which was not statistically limited (i.e., where there are events compatible with the SM background), where  $D$  is the ratio of the full integrated luminosity of  $139 \text{ fb}^{-1}$  that was collected by the end of Run II [55, 56], to the already analyzed integrated luminosity of  $36.1 \text{ fb}^{-1}$  in the ATLAS experiment. It is clear that further improvement on the constraining of this mixing can be achieved from the analysis of such data. At fixed  $M_{W'}$  the exclusion constraint on  $\xi$  scales as  $\sim \mathcal{L}_{\text{int}}^{-1/4}$  when statistical errors dominate. The increase of the time-integrated luminosity from  $36.1 \text{ fb}^{-1}$  to  $139 \text{ fb}^{-1}$  will allow to set stronger constraints on the mixing angle  $\xi$  by a factor of  $\simeq 1.4$ .<sup>5</sup> We find that the LHC limits obtained at 13 TeV and time-integrated luminosity,  $\mathcal{L}_{\text{int}} = 36.1 \text{ fb}^{-1}$ , already improves on the EW limits approximately by one order of magnitude.

Further improvement in placing limits on the  $W'$  mass and  $W$ - $W'$  mixing parameter is feasible in fully-hadronic  $WZ \rightarrow qqqq$  final states using the full Run II data set [56]. The recent analysis performed in [56] is able to largely improve on the results above for  $\sim 36 \text{ fb}^{-1}$ , mostly due to the use of novel reconstruction and analysis techniques. Our fast and approximate estimation based on the full (preliminary) Run II data set shows that the improvement in expected upper limits on  $\xi$  for the  $WZ$  channel at  $\sim 3 \text{ TeV}$  is about a factor of two smaller than that presented here. However, a detailed analysis of the  $W$ - $W'$  mixing effects in the fully-hadronic  $WZ \rightarrow qqqq$  final states is beyond the scope of the present paper and will be presented elsewhere.

## V. CONCLUDING REMARKS

Exploration of the the diboson  $WZ$  and dilepton  $e\nu$  production at the LHC with the 13 TeV data set allows to place stringent constraints on the  $W$ - $W'$  mixing angle and  $W'$  mass,  $M_{W'}$ . We derived such limits by using data recorded by the ATLAS detector at the CERN LHC, with integrated luminosity of  $\sim 36.1 \text{ fb}^{-1}$ . By comparing the experimental limits to the theoretical predictions for the total cross section of  $W'$  resonant production and its subsequent decay into  $WZ$  and  $e\nu$  pairs, we show that the derived constraints on the  $W$ - $W'$  mixing angle for the EGM model are substantially improved with respect to those obtained from the global analysis of low energy electroweak data, as well as from the diboson production study performed at the Tevatron and those based on the LHC Run I. Further constraining of this mixing can be achieved from the analysis of data already collected by the end of Run II, still to be analyzed. The new LHC bound starts to become highly competitive with the constraints coming from low-energy EW studies and after the LHC Run I.

In addition, our work shows that accounting for the contribution of the  $W'$  boson decay channel,  $W' \rightarrow WH$ , to the total width  $\Gamma_{W'}$  does not dramatically affect the bounds on the mixing parameter  $\xi$  obtained in the scenario of a vanishing  $WH$  mode. Namely, it turns out that for the higher  $W'$  masses the constraints on  $W$ - $W'$  mixing are relaxed by a few relative percent for the  $WZ$  channel as illustrated in Fig. 6. One should also note that in this paper, for the sake of compactness of the graphic material, we limited ourselves to an analysis of experimental data from the ATLAS detector only. Our further analysis shows that the corresponding CMS data [53, 57, 58] yields bounds on the mixing parameter  $\xi$  and the  $W'$  boson mass that agree with the results based on the ATLAS data.

---

<sup>5</sup> Such scaling law is also adopted for evaluation of the  $Z$ - $Z'$  mixing strength vs  $\mathcal{L}_{\text{int}}$  in the process  $pp \rightarrow Z'X \rightarrow W^+W^-X$  [28, 29].

## ACKNOWLEDGEMENTS

We would like to thank V. A. Bednyakov for helpful discussions. This research has been partially supported by the Abdus Salam ICTP (TRIL Programme). The work of PO has been supported by the Research Council of Norway.

- 
- [1] M. Tanabashi *et al.* [Particle Data Group], “Review of Particle Physics,” *Phys. Rev. D* **98**, no. 3, 030001 (2018). doi:10.1103/PhysRevD.98.030001
  - [2] G. Altarelli, B. Mele and M. Ruiz-Altaba, “Searching for New Heavy Vector Bosons in  $p\bar{p}$  Colliders,” *Z. Phys. C* **45**, 109 (1989) Erratum: [*Z. Phys. C* **47**, 676 (1990)]. doi:10.1007/BF01552335, 10.1007/BF01556677
  - [3] M. Aaboud *et al.* [ATLAS Collaboration], “Search for a new heavy gauge boson resonance decaying into a lepton and missing transverse momentum in 36 fb<sup>-1</sup> of  $pp$  collisions at  $\sqrt{s} = 13$  TeV with the ATLAS experiment,” *Eur. Phys. J. C* **78**, no. 5, 401 (2018) doi:10.1140/epjc/s10052-018-5877-y [arXiv:1706.04786 [hep-ex]].
  - [4] A. M. Sirunyan *et al.* [CMS Collaboration], “Search for high-mass resonances in final states with a lepton and missing transverse momentum at  $\sqrt{s} = 13$  TeV,” *JHEP* **1806**, 128 (2018) doi:10.1007/JHEP06(2018)128 [arXiv:1803.11133 [hep-ex]].
  - [5] M. Schmaltz and C. Spethmann, “Two Simple  $W'$  Models for the Early LHC,” *JHEP* **1107**, 046 (2011) doi:10.1007/JHEP07(2011)046 [arXiv:1011.5918 [hep-ph]].
  - [6] C. Grojean, E. Salvioni and R. Torre, “A weakly constrained  $W'$  at the early LHC,” *JHEP* **1107**, 002 (2011) doi:10.1007/JHEP07(2011)002 [arXiv:1103.2761 [hep-ph]].
  - [7] E. E. Boos, I. P. Volobuev, M. A. Perfilov and M. N. Smolyakov, “Searches for  $W'$  and  $Z'$  in Models with Large Extra Dimensions,” *Theor. Math. Phys.* **170** (2012) 90 doi:10.1007/s11232-012-0009-6 [arXiv:1106.2400 [hep-ph]].
  - [8] T. Jezo, M. Klasen and I. Schienbein, “LHC phenomenology of general  $SU(2)_C \times SU(2)_F \times U(1)$  models,” *Phys. Rev. D* **86**, 035005 (2012) doi:10.1103/PhysRevD.86.035005 [arXiv:1203.5314 [hep-ph]].
  - [9] Q. H. Cao, Z. Li, J. H. Yu and C. P. Yuan, “Discovery and Identification of  $W'$  and  $Z'$  in  $SU(2)_C \times SU(2)_F \times U(1)$  Models at the LHC,” *Phys. Rev. D* **86**, 095010 (2012) doi:10.1103/PhysRevD.86.095010 [arXiv:1205.3769 [hep-ph]].
  - [10] B. A. Dobrescu and Z. Liu, “Heavy Higgs bosons and the 2 TeV  $W'$  boson,” *JHEP* **1510**, 118 (2015) doi:10.1007/JHEP10(2015)118 [arXiv:1507.01923 [hep-ph]].
  - [11] P. S. Bhupal Dev and R. N. Mohapatra, “Unified explanation of the  $eejj$ , diboson and dijet resonances at the LHC,” *Phys. Rev. Lett.* **115**, no. 18, 181803 (2015) doi:10.1103/PhysRevLett.115.181803 [arXiv:1508.02277 [hep-ph]].
  - [12] E. E. Boos, V. E. Bunichev, M. A. Perfilov, M. N. Smolyakov and I. P. Volobuev, “The specificity of searches for  $W'$ ,  $Z'$  and  $\gamma'$  coming from extra dimensions,” *JHEP* **1406**, 160 (2014) doi:10.1007/JHEP06(2014)160 [arXiv:1311.5968 [hep-ph]].
  - [13] A. Baskakov, E. Boos, V. Bunichev, M. Perfilov and I. Volobuev, “Restrictions on the mass of the KK excitation  $W'$  from the Higgs boson diphoton decay and the single top production,” *EPJ Web Conf.* **191**, 02007 (2018). doi:10.1051/epjconf/201819102007
  - [14] N. Bakhet, T. Hussein and M. Y. Khlopov, “Search for New Charged Gauge Boson  $W'$  via Phenomenology of the Left-Right Symmetric Model at Hadron Colliders,” *International Journal of Theoretical and Applied Physics (IJTAP)*, Vol.4, p. 51 (2014) [arXiv:1406.3254 [hep-ph]].
  - [15] E. Eichten, I. Hinchliffe, K. D. Lane and C. Quigg, “Super Collider Physics,” *Rev. Mod. Phys.* **56**, 579 (1984) Addendum: [*Rev. Mod. Phys.* **58**, 1065 (1986)]. doi:10.1103/RevModPhys.56.579, 10.1103/RevModPhys.58.1065
  - [16] L. Randall and R. Sundrum, “A Large mass hierarchy from a small extra dimension,” *Phys. Rev. Lett.* **83**, 3370 (1999) doi:10.1103/PhysRevLett.83.3370 [hep-ph/9905221].
  - [17] H. Davoudiasl, J. L. Hewett and T. G. Rizzo, “Experimental probes of localized gravity: On and off the wall,” *Phys. Rev. D* **63**, 075004 (2001) doi:10.1103/PhysRevD.63.075004 [hep-ph/0006041].
  - [18] K. Lane and S. Mrenna, “The Collider phenomenology of technihadrons in the technicolor straw man model,” *Phys. Rev. D* **67**, 115011 (2003) doi:10.1103/PhysRevD.67.115011 [hep-ph/0210299].
  - [19] E. Eichten and K. Lane, “Low-scale technicolor at the Tevatron and LHC,” *Phys. Lett. B* **669**, 235 (2008) doi:10.1016/j.physletb.2008.09.047 [arXiv:0706.2339 [hep-ph]].
  - [20] K. Agashe, R. Contino and A. Pomarol, “The Minimal composite Higgs model,” *Nucl. Phys. B* **719**, 165 (2005) doi:10.1016/j.nuclphysb.2005.04.035 [hep-ph/0412089].
  - [21] G. F. Giudice, C. Grojean, A. Pomarol and R. Rattazzi, “The Strongly-Interacting Light Higgs,” *JHEP* **0706**, 045 (2007) doi:10.1088/1126-6708/2007/06/045 [hep-ph/0703164].
  - [22] D. Liu, L. T. Wang and K. P. Xie, “Prospects of searching for composite resonances at the LHC and beyond,” *JHEP* **1901**, 157 (2019) doi:10.1007/JHEP01(2019)157 [arXiv:1810.08954 [hep-ph]].
  - [23] H. J. He *et al.*, “CERN LHC Signatures of New Gauge Bosons in Minimal Higgsless Model,” *Phys. Rev. D* **78**, 031701 (2008) doi:10.1103/PhysRevD.78.031701 [arXiv:0708.2588 [hep-ph]].
  - [24] F. De Guio, “Search for a heavy gauge boson  $W'$  in the final state with electron and large  $E_T^{miss}$  in  $pp$  collisions at  $\sqrt{s} = 7$  TeV,” CERN-THESIS-2012-425.
  - [25] G. Aad *et al.* [ATLAS Collaboration], “Search for resonant diboson production in the  $\ell\ell q\bar{q}$  final state in  $pp$  collisions at  $\sqrt{s} = 8$  TeV with the ATLAS detector,” *Eur. Phys. J. C* **75**, 69 (2015) doi:10.1140/epjc/s10052-015-3261-8 [arXiv:1409.6190 [hep-ex]].

- [26] G. Aad *et al.* [ATLAS Collaboration], “Combination of searches for  $WW$ ,  $WZ$ , and  $ZZ$  resonances in  $pp$  collisions at  $\sqrt{s} = 8$  TeV with the ATLAS detector,” *Phys. Lett. B* **755**, 285 (2016) doi:10.1016/j.physletb.2016.02.015 [arXiv:1512.05099 [hep-ex]].
- [27] V. V. Andreev, P. Osland and A. A. Pankov, “Precise determination of  $Z$ - $Z'$  mixing at the CERN LHC,” *Phys. Rev. D* **90**, no. 5, 055025 (2014) doi:10.1103/PhysRevD.90.055025 [arXiv:1406.6776 [hep-ph]].
- [28] P. Osland, A. A. Pankov and A. V. Tsytrinov, “Probing  $Z$ - $Z'$  mixing with ATLAS and CMS resonant diboson production data at the LHC at  $\sqrt{s} = 13$  TeV,” *Phys. Rev. D* **96**, no. 5, 055040 (2017) doi:10.1103/PhysRevD.96.055040 [arXiv:1707.02717 [hep-ph]].
- [29] I. D. Bobovnikov, P. Osland and A. A. Pankov, “Improved constraints on the mixing and mass of  $Z'$  bosons from resonant diboson searches at the LHC at  $\sqrt{s} = 13$  TeV and predictions for Run II,” *Phys. Rev. D* **98**, no. 9, 095029 (2018) doi:10.1103/PhysRevD.98.095029 [arXiv:1809.08933 [hep-ph]].
- [30] T. Aaltonen *et al.* [CDF Collaboration], “Search for  $WW$  and  $WZ$  resonances decaying to electron, missing  $E_T$ , and two jets in  $p\bar{p}$  collisions at  $\sqrt{s} = 1.96$  TeV,” *Phys. Rev. Lett.* **104**, 241801 (2010) doi:10.1103/PhysRevLett.104.241801 [arXiv:1004.4946 [hep-ex]].
- [31] M. Aaboud *et al.* [ATLAS Collaboration], “Search for  $WW/WZ$  resonance production in  $\ell\nu qq$  final states in  $pp$  collisions at  $\sqrt{s} = 13$  TeV with the ATLAS detector,” *JHEP* **1803**, 042 (2018) doi:10.1007/JHEP03(2018)042 [arXiv:1710.07235 [hep-ex]].
- [32] V. M. Abazov *et al.* [D0 Collaboration], “Search for a resonance decaying into  $WZ$  boson pairs in  $p\bar{p}$  collisions,” *Phys. Rev. Lett.* **104**, 061801 (2010) doi:10.1103/PhysRevLett.104.061801 [arXiv:0912.0715 [hep-ex]].
- [33] G. Aad *et al.* [ATLAS Collaboration], “Search for  $WZ$  resonances in the fully leptonic channel using  $pp$  collisions at  $\sqrt{s} = 8$  TeV with the ATLAS detector,” *Phys. Lett. B* **737**, 223 (2014) doi:10.1016/j.physletb.2014.08.039 [arXiv:1406.4456 [hep-ex]].
- [34] V. Khachatryan *et al.* [CMS Collaboration], “Search for new resonances decaying via  $WZ$  to leptons in proton-proton collisions at  $\sqrt{s} = 8$  TeV,” *Phys. Lett. B* **740**, 83 (2015) doi:10.1016/j.physletb.2014.11.026 [arXiv:1407.3476 [hep-ex]].
- [35] G. Aad *et al.* [ATLAS Collaboration], “Search for production of  $WW/WZ$  resonances decaying to a lepton, neutrino and jets in  $pp$  collisions at  $\sqrt{s} = 8$  TeV with the ATLAS detector,” *Eur. Phys. J. C* **75**, no. 5, 209 (2015) Erratum: [*Eur. Phys. J. C* **75**, 370 (2015)] doi:10.1140/epjc/s10052-015-3593-4, 10.1140/epjc/s10052-015-3425-6 [arXiv:1503.04677 [hep-ex]].
- [36] G. Aad *et al.* [ATLAS Collaboration], “Search for high-mass diboson resonances with boson-tagged jets in proton-proton collisions at  $\sqrt{s} = 8$  TeV with the ATLAS detector,” *JHEP* **1512**, 055 (2015) doi:10.1007/JHEP12(2015)055 [arXiv:1506.00962 [hep-ex]].
- [37] V. Khachatryan *et al.* [CMS Collaboration], “Search for massive resonances in dijet systems containing jets tagged as  $W$  or  $Z$  boson decays in  $pp$  collisions at  $\sqrt{s} = 8$  TeV,” *JHEP* **1408**, 173 (2014) doi:10.1007/JHEP08(2014)173 [arXiv:1405.1994 [hep-ex]].
- [38] D. Pappadopulo, A. Thamm, R. Torre and A. Wulzer, “Heavy Vector Triplets: Bridging Theory and Data,” *JHEP* **1409**, 060 (2014) doi:10.1007/JHEP09(2014)060 [arXiv:1402.4431 [hep-ph]].
- [39] G. Aad *et al.* [ATLAS Collaboration], “Search for resonant diboson production in the  $WW/WZ \rightarrow \ell\nu jj$  decay channels with the ATLAS detector at  $\sqrt{s} = 7$  TeV,” *Phys. Rev. D* **87**, no. 11, 112006 (2013) doi:10.1103/PhysRevD.87.112006 [arXiv:1305.0125 [hep-ex]].
- [40] S. Chatrchyan *et al.* [CMS Collaboration], “Search for a  $W'$  or Techni- $\rho$  Decaying into  $WZ$  in  $pp$  Collisions at  $\sqrt{s} = 7$  TeV,” *Phys. Rev. Lett.* **109**, 141801 (2012) doi:10.1103/PhysRevLett.109.141801 [arXiv:1206.0433 [hep-ex]].
- [41] V. D. Barger and R. J. N. Phillips, “Collider Physics,” Addison-Wesley (1987), Redwood City, USA (Frontiers in Physics, vol. 71).
- [42] E. Nuss, “Diboson production at hadron colliders with general three gauge boson couplings. Analytic expressions of helicity amplitudes and cross-section,” *Z. Phys. C* **76**, 701 (1997) doi:10.1007/s002880050592 [hep-ph/9610309].
- [43] J. Pumplin, D. R. Stump, J. Huston, H. L. Lai, P. M. Nadolsky and W. K. Tung, “New generation of parton distributions with uncertainties from global QCD analysis,” *JHEP* **0207**, 012 (2002) doi:10.1088/1126-6708/2002/07/012 [hep-ph/0201195].
- [44] G. Aad *et al.* [ATLAS Collaboration], “Search for new particles in events with one lepton and missing transverse momentum in  $pp$  collisions at  $\sqrt{s} = 8$  TeV with the ATLAS detector,” *JHEP* **1409**, 037 (2014) doi:10.1007/JHEP09(2014)037 [arXiv:1407.7494 [hep-ex]].
- [45] M. S. Chanowitz and M. K. Gaillard, “The TeV Physics of Strongly Interacting  $W$ ’s and  $Z$ ’s,” *Nucl. Phys. B* **261**, 379 (1985). doi:10.1016/0550-3213(85)90580-2
- [46] M. Aaboud *et al.* [ATLAS Collaboration], “Searches for heavy diboson resonances in  $pp$  collisions at  $\sqrt{s} = 13$  TeV with the ATLAS detector,” *JHEP* **1609**, 173 (2016) doi:10.1007/JHEP09(2016)173 [arXiv:1606.04833 [hep-ex]].
- [47] A. M. Sirunyan *et al.* [CMS Collaboration], “Combination of searches for heavy resonances decaying to  $WW$ ,  $WZ$ ,  $ZZ$ ,  $WH$ , and  $ZH$  boson pairs in proton-proton collisions at  $\sqrt{s} = 8$  and 13 TeV,” *Phys. Lett. B* **774**, 533 (2017) doi:10.1016/j.physletb.2017.09.083 [arXiv:1705.09171 [hep-ex]].
- [48] T. Sjostrand *et al.*, “An Introduction to PYTHIA 8.2,” *Comput. Phys. Commun.* **191**, 159 (2015) doi:10.1016/j.cpc.2015.01.024 [arXiv:1410.3012 [hep-ph]].
- [49] R. Hamberg, W. L. van Neerven and T. Matsuura, “A complete calculation of the order  $\alpha_s^2$  correction to the Drell-Yan  $K$  factor,” *Nucl. Phys. B* **359**, 343 (1991) Erratum: [*Nucl. Phys. B* **644**, 403 (2002)]. doi:10.1016/S0550-3213(02)00814-3, 10.1016/0550-3213(91)90064-5
- [50] A. Alves, O. J. P. Eboli, D. Goncalves, M. C. Gonzalez-Garcia and J. K. Mizukoshi, “Signals for New Spin-1 Resonances in Electroweak Gauge Boson Pair Production at the LHC,” *Phys. Rev. D* **80**, 073011 (2009)

- doi:10.1103/PhysRevD.80.073011 [arXiv:0907.2915 [hep-ph]].
- [51] R. Gavin, Y. Li, F. Petriello and S. Quackenbush, “FEWZ 2.0: A code for hadronic Z production at next-to-next-to-leading order,” *Comput. Phys. Commun.* **182**, 2388 (2011) doi:10.1016/j.cpc.2011.06.008 [arXiv:1011.3540 [hep-ph]].
  - [52] Y. Li and F. Petriello, “Combining QCD and electroweak corrections to dilepton production in FEWZ,” *Phys. Rev. D* **86**, 094034 (2012) doi:10.1103/PhysRevD.86.094034 [arXiv:1208.5967 [hep-ph]].
  - [53] V. Khachatryan *et al.* [CMS Collaboration], “Search for heavy gauge  $W'$  boson in events with an energetic lepton and large missing transverse momentum at  $\sqrt{s} = 13$  TeV,” *Phys. Lett. B* **770**, 278 (2017) doi:10.1016/j.physletb.2017.04.043 [arXiv:1612.09274 [hep-ex]].
  - [54] The ATLAS collaboration [ATLAS Collaboration], “Search for a new heavy gauge boson resonance decaying into a lepton and missing transverse momentum in  $79.8 \text{ fb}^{-1}$  of  $pp$  collisions at  $\sqrt{s} = 13$  TeV with the ATLAS experiment,” ATLAS-CONF-2018-017.
  - [55] The ATLAS collaboration [ATLAS Collaboration], “Search for high-mass dilepton resonances using  $139 \text{ fb}^{-1}$  of  $pp$  collision data collected at  $\sqrt{s} = 13$  TeV with the ATLAS detector,” ATLAS-CONF-2019-001.
  - [56] The ATLAS collaboration [ATLAS Collaboration], “Search for diboson resonances in hadronic final states in  $139 \text{ fb}^{-1}$  of  $pp$  collisions at  $\sqrt{s} = 13$  TeV with the ATLAS detector,” ATLAS-CONF-2019-003.
  - [57] A. M. Sirunyan *et al.* [CMS Collaboration], “Search for massive resonances decaying into  $WW$ ,  $WZ$ ,  $ZZ$ ,  $qW$ , and  $qZ$  with dijet final states at  $\sqrt{s} = 13$  TeV,” *Phys. Rev. D* **97**, no. 7, 072006 (2018) doi:10.1103/PhysRevD.97.072006 [arXiv:1708.05379 [hep-ex]].
  - [58] A. M. Sirunyan *et al.* [CMS Collaboration], “Search for a heavy resonance decaying into a Z boson and a Z or W boson in  $2\ell 2q$  final states at  $\sqrt{s} = 13$  TeV,” *JHEP* **1809**, 101 (2018) doi:10.1007/JHEP09(2018)101 [arXiv:1803.10093 [hep-ex]].